

Hot switching damage mechanisms in MEMS contacts – evidence and understanding

Anirban Basu¹, Ryan P Hennessy², George G Adams^{2,4}, and Nicol E McGruer^{1,3}

1) Department of Electrical and Computer Engineering, Northeastern University, Boston, MA 02115, USA

2) Department of Mechanical and Industrial Engineering, Northeastern University, Boston, MA 02115, USA

3) Email: mcgruer@ece.neu.edu

4) Email: adams@coe.neu.edu

Abstract. Using an AFM-based test setup, experiments were performed on Ru microcontacts under a variety of leading and trailing edge hot switching conditions, including different voltages, different currents, different polarities (including bipolar and ac up to 20 MHz), and different approach and separation rates. It was found that hot switching damage is a complex phenomenon for microcontacts. It consists of a number of different mechanisms occurring simultaneously to different degrees depending on the hot switching conditions. It was determined through a combination of experiments and models that the mechanisms leading to contact erosion operate when the electrodes are separated by less than a few Å or are barely touching. For leading edge hot switching, i.e. hot switching when the contacts are closing, the main damage mechanism was found to be associated with currents less than 0.15 mA. Pre-contact currents were observed on uncleaned contacts and were not found to contribute to contact damage. Despite the damage caused by hot switching, it was found that unless the contact material is almost or completely eroded, hot switching does not lead to high contact resistance or high adhesion on Ru contacts. Under bipolar hot switching conditions, microcontacts with a 400 μN contact force maintained a contact resistance of less than 1 Ω and a pull-off force less than 60 μN for more than 100 million cycles.

Key Words: MEMS switches, Contacts, Hot Switching, Material transfer, Contact Damage, Adhesion

1. Introduction

Metal contact RF MEMS switches have received attention lately due to their potential applications in communications [1], general switching [2] and digital logic [3]. Metal contact switches have low on-resistance, high isolation, and are suitable for signals with frequencies ranging from dc to millimeter wave (100 GHz) and beyond [4,5,6,7,8]. The reliability of metal contact MEMS switches is in large part related to the reliability of their electrical contacts. MEMS contacts are also important for devices such as probe cards [9,10,11] where understanding the contact properties can lead to a more informed choice of contact material for the structures. The performance and reliability of MEMS contacts under hot switched conditions is an area that has been relatively unexplored. However it needs to be addressed, particularly in

light of the discoveries discussed below that the amount of contact damage does not vary monotonically with voltage and that under typical switching conditions, Ru contacts can operate reliably for more than 10^8 cycles.

For this work, the contact material is Ru. Previous research has investigated the performance of electrical contacts coated with different materials under cold switching and mechanical cycling conditions. In Au contacts, adhesion was found to be a major issue leading to contacts sticking closed [12]. Au alloys, with better hardness and lower adhesion, were also investigated [13]. Pt, Ir, Ru, Au, and Au alloys were compared [14,15]. Of these materials, Ru contacts which have undergone oxygen plasma cleaning and have a thin layer of ruthenium oxide have shown excellent performance under cold switching conditions, being resistant to contamination as well as having very low adhesion [15,16].

MEMS switch contact damage is observed in cold switching due to adhesion (stuck closed) and carbon contamination (stuck open). However, it is hot switching that causes the most damage to metal contacts as has been shown and discussed earlier [17,18]. Hot switching refers to the application of a voltage (dc, ac, or RF) across the switch contacts during its transition process from open to closed and vice versa. Although it is sometimes possible to design systems to avoid hot switching, it is often desirable or essential for switches to be able to withstand some amount of hot switching without significant damage or degradation in performance. This is true in many RF and power applications, as well as in potential digital logic applications.

Hot switching damage in microcontacts has been analyzed from various perspectives by different research groups. In the late 90s, MEMS contacts were studied as a part of the overall study of reliability of MEMS switches. It was deduced early on that in the absence of the high voltages associated with arcs, the damage mechanisms for the MEMS relays have to be different from contact damage in macrorelays [19]. More investigation of damage mechanisms and damage characteristics in MEMS switches was not undertaken until a few years back. This group reported that hot switching at the leading and trailing edges, and for positive and negative polarities, leads to transfer of about 500 nm^3 of material per cycle from the anode to the cathode [20]. In [17], contact damage was associated with current transients due to parasitic inductances in the circuit which can be compensated for by adding a capacitive quenching circuit. Field emission and field evaporation have been suggested by two research groups as damage mechanisms [21,22,23]. The field emission theory proposes that at small distances, tunneling of electrons occurs from cathode to anode. Tunneling electrons transfer energy to the anode, causing the temperature to rise. If the temperature of the hottest area of the anode is high enough, then material from the anode will evaporate and deposit on the cathode. On the other hand, field evaporation theory suggests that the electric field between the contacts at small separations can directly cause atoms to be pulled out of the anode lattice and transferred to the cathode.

There are other possible material transfer mechanisms that can lead to contact erosion. One mechanism is the formation of a metal vapor when asperities come into contact and then evaporate due to the high temperature associated with high contact voltages. If the metal vapor is ionized, the positively charged ions are attracted towards the cathode leading to mass transfer in the direction of the electric field [24,25]. At the trailing edge, there is the possibility of formation of a metal bridge [26,27] which subsequently evaporates due to the high associated temperature, forming a metal vapor that ionizes and finally gets deposited on to the cathode. There is also the possibility of material transfer due to electromigration at the extremely high current densities in the contact. Such electromigration can be accelerated due to the formation of a molten bridge [28]. Thermal effects, such as the Thomson effect where the flow of current causes a thermal gradient in a molten bridge, which in turn leads to material being transferred towards the cooler electrode, can also lead to material transfer which is polarity-dependent [29].

This work builds on the previous work presented in [20]. In order to understand the complexity of hot switching damage mechanisms, switches were tested under a variety of conditions. In the following sections, the experimental setup is first described briefly including a description of the capabilities of the system. This is followed by the different test results which demonstrate the presence of multiple mechanisms during hot switching. The results include observation of four distinct regimes associated

with hot switching at different voltages, polarity dependent and polarity independent material transfer, presence/absence of pre-contact current spikes, lack of association of pre-contact current with material transfer, hot switching damage at reduced approach and separation rates, bipolar hot switching damage, hot switching with different external resistances and hot switching with AC voltages up to 20 MHz. A combination of experiments and models are used to understand which material transfer mechanisms may be active.

2. Experimental Setup

For study of MEMS contacts, several research groups have in the past built contact testers. Some of the contact test setups that have been used by research groups include – 1) Pico-indenter [30], 2) Nano-indenter [31,32], 3) Customized AFM setup [33], 4) Piezoresistive cantilever, nanopositioner and an interferometer for displacement measurement [34] and 5) a customized station using force sensor and piezo-motor [35]. With most systems, particularly the nano and pico-indenters, there is a compromise between accuracy and speed of testing. Cycling the contacts for more than 10^6 cycles requires that cycling be performed at a fast enough rate so that the test does not prolong to days. For this purpose, an AFM-based tester proved to be very useful. A detailed description of the setup can be found in [20] but a brief description is presented below to highlight the important functions of the system.

The contact pair consists of a contact bump at the center of a clamped-clamped beam force measurement structure and a mating pillar. The force measurement structure is housed in a chip that is located where the AFM cantilever tip is usually placed. This chip is stationary. The pillar is placed on a piezoelectric actuator (Physik Instrumente PL022.31) which is placed on the base of the AFM, so that the pillar can be accurately positioned by the AFM. The piezoelectric actuator then allows rapid cycling of the contact bump and the pillar in and out of contact. The contact force and contact resistance are measured simultaneously in the test setup. The deflection of the laser beam in the AFM during a switching cycle is calibrated to measure the contact force. The contact bump chip and the pillar chip are configured for 4-wire resistance measurements. **Figure 1** shows a schematic of the resistance measurement setup. Nitrogen is flown into the AFM chamber when the tests are conducted in order to ensure a relatively clean atmosphere during the course of lifetime tests.

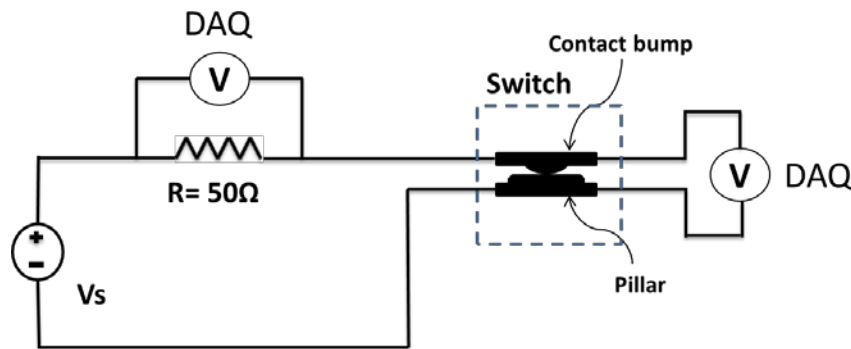


Figure 1. Schematic of the four-probe contact resistance measurement setup. R is typically 50 Ohms, but both V_s and R are varied for measurements over a range of voltages and currents.

The contact resistance can be determined from the measured voltages across the 50Ω resistor and the contact as:

$$R_C = \frac{V_C}{V_R} R_R$$

where V_R is the voltage across the external resistor, V_C is the voltage across the contact, and R_R is the external resistance which is 50Ω .

2.1. Capabilities of the test setup

Many of the capabilities of this AFM-based tester are automated using LabVIEW. There are three voltages applied to the tester. One is the voltage to the series combination of the contact and the resistor. The second is the voltage across the piezoelectric actuator. A third, slowly varying voltage, is computed from the measured waveforms and applied to the AFM piezo to compensate for drift in the AFM during long tests.

The testing described below uses the following capabilities:

- The actuation waveform for switching cycles can be controlled as required. A ramp-hold-ramp voltage is usually applied. The ramping speed is $4400 \mu\text{m/s}$ for most tests, but other velocities were used as described below. The LabVIEW program can be used for cold switching, hot switching (including leading edge or trailing edge hot switching with either polarity or with alternating polarities). **Figure 2** shows some of the hot switching cycles used in this work.
- A separate LabVIEW program was used for extremely slow cycling, with contact approach/withdrawal velocities of a few nm/s.

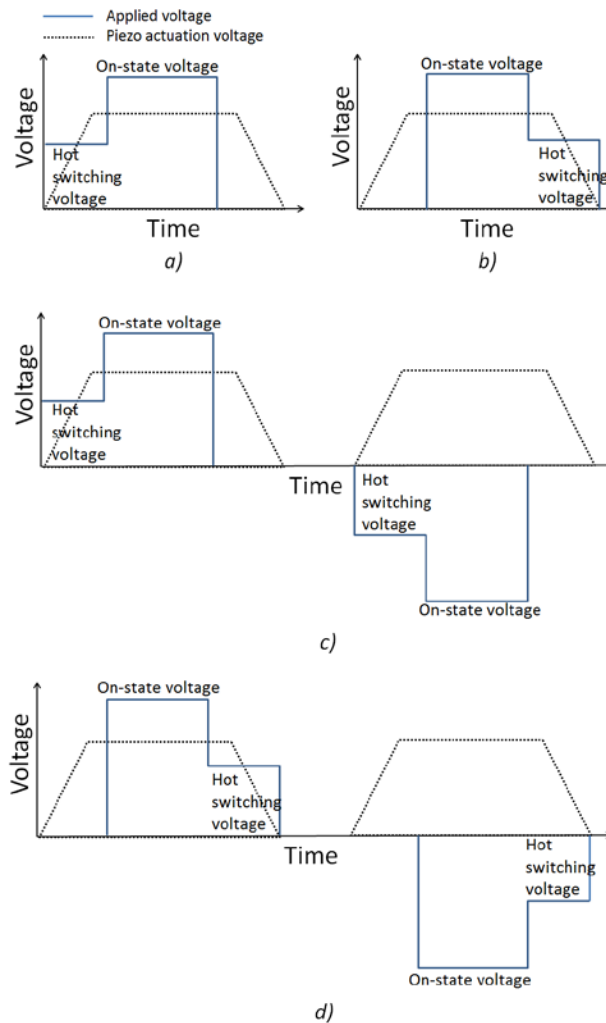


Figure 2. Schematics of the voltage waveforms associated with the four different hot switching modes discussed. a) Leading edge unipolar hot switching, b) Trailing edge unipolar hot switching, c) Leading edge bipolar hot switching, d) Trailing edge bipolar hot switching.

3. Test results and discussion

3.1 Complexity of hot switching damage – The results in this paper show that hot switching MEMS contact damage is a complex phenomenon which cannot be explained through any single mechanism. The following results demonstrate that hot switching damage mechanisms change depending on operating conditions:

- 1) For different hot switching voltages between 0 V (cold switched) to 3.5 V, there are differences in the amount of damage on the microcontacts. It was found that cold switching results in very little damage, 0.25 V causes more damage than cold switching. 0.5 V results in both more damage and a change in the character of the damage, with much more material scatter. Hot switching at 1.0 V or 2.0 V results in less material scatter, with small amounts of apparently randomly-directed material transfer. Finally, 3.5 V hot switching consistently leads to a relatively large amount of material transfer from the anode to the cathode. At 3.5 V, leading edge hot switching causes more material scatter than trailing edge hot switching.
- 2) At 5.0 V, with a slow separation rate of 8.8 nm/s, material transfer is polarity independent and always from the contact bump and toward the pillar.
- 3) Bipolar hot switching leads to very slow material transfer from the contact bump to the pillar.
- 4) Under low external resistance conditions, leading edge and trailing edge hot switching lead to similar amounts of material transfer [20], but under high external resistance conditions, leading and trailing edge hot switching lead to different amounts of material transfer.
- 5) Material transfer from anode to cathode often leads to conformal shaped pits and mounds on either end of the contact. However, this is not found to be true when large amounts of material scatter are observed, for example at 0.5 V and often during leading edge hot switching at 3.5 V.

3.2 Hot switching damage at different voltages – To understand hot switching mechanisms, tests were conducted for both leading and trailing edge hot switching with the contact bump as either anode or cathode, at hot switching voltages ranging from 0 to 3.5 V. The images in **Figure 3** and **Figure 4** show typical results under these conditions. All the tested contacts were cycled up to 10^6 cycles.

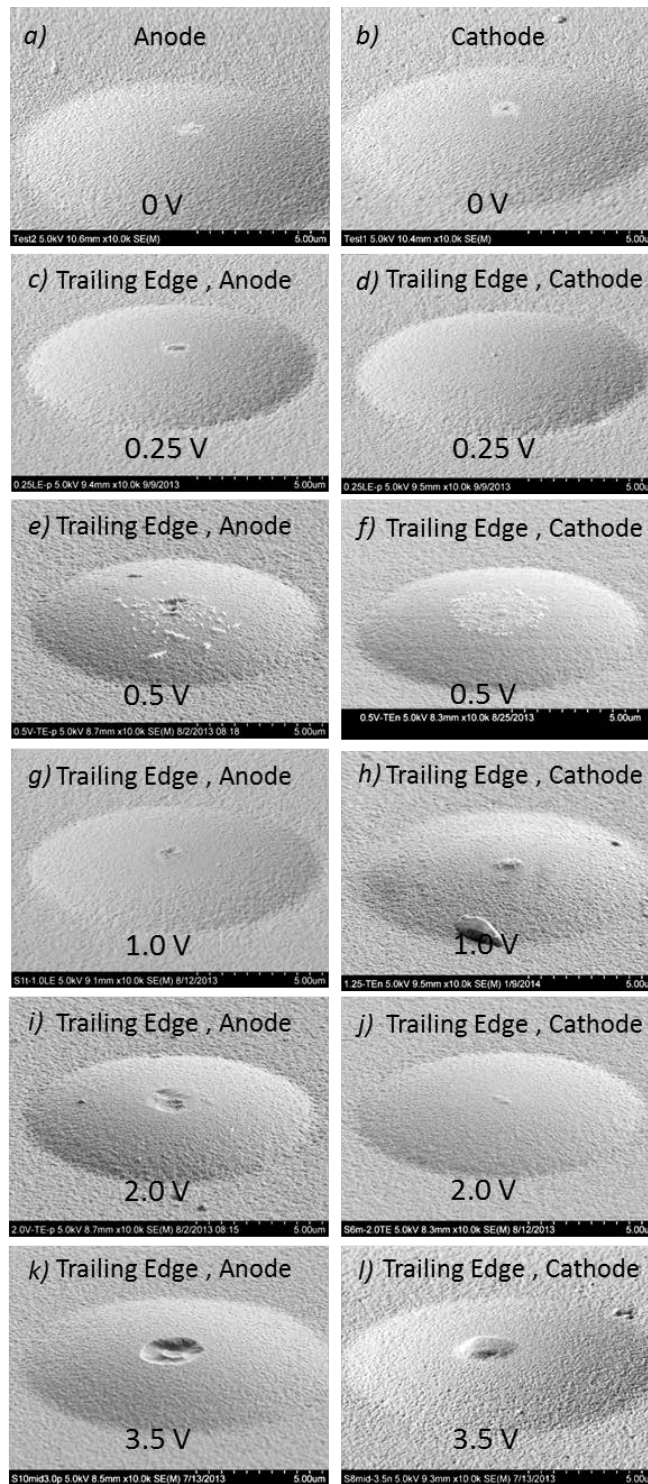


Figure 3. Trailing edge hot switching contact bump damage at different voltages after 10^6 cycles. The on-state current was 77.5 mA for all except the 0V tests.

In **Figure 3**, different types of trailing edge hot switching contact damage at several voltages are shown when the contact bump is either the anode or the cathode. It is noted that 0.25 V of hot switching voltage causes very little damage either comparable to cold switching or, as seen later in **Figure 4**,

sometimes more than cold switching. At 0.5 V, there appears to be contact damage that is much more severe than at either 0.25 V or 1.0 V. This result was found to be very consistent, occurring in all contacts tested at 0.5 V. At 1.0 and 2.0 V, there is no clear trend in material transfer direction although material scatter is much less. At 3.5 V the direction of material transfer is always from anode to cathode. It should also be noted that pronounced material scatter sometimes accompanies material transfer for leading edge hot switching at a hot switching voltage of 3.5 V, as shown in Figure 4 (k) and (l). This phenomenon is never observed for trailing edge hot switching.

Tests were performed for leading edge hot switching as shown in **Figure 4**. Again, at 0.5 V, the enhanced material scatter is seen, suggesting that a similar damage mechanism is present for both leading and trailing edge switching at this voltage. At 1.0 V and 2.0 V, small quantities of material transfer are observed with no clear trend in direction. This points to a mechanism that is either random or that there is material transfer in both directions but for a given test, we end up getting more material transfer in one direction as opposed to the other. This appears to be a statistical phenomenon. At 3.5 V, the material transfer is polarity dependent and always from anode to cathode, similar to leading edge hot switching. With the exception of the sometimes different appearance of leading-edge hot switching damage at 3.5 V shown in **Figure**

4, these results support the idea that the contact damage mechanisms at the leading and trailing edges are similar, at least over this range of conditions. Later we will highlight conditions that lead to different results for leading and trailing edge hot switching. Also, in an earlier paper by this group [20], it was stated that trailing edge hot switching leads to a higher pull-off force between the contacts. This effect was subsequently found to be caused by the force structures bending due to joule heating during opening of the contact.

The melting voltage of Ru is around 0.8 V. This can be deduced using the following relationship between contact voltage and contact temperature given in [29]:

$$V_c = \sqrt{4L_0(T_c^2 - T_0^2)}$$

L_0 is Lorentz's constant, T_c is the contact temperature and T_0 is the temperature at a point far away from the contact (ambient). The melting temperature of Ru is 2607 K. If the product of thermal conductivity and electrical resistivity remain constant beyond melting, then the boiling voltage can be estimated to be around 1.5 V (boiling temperature for Ru is 4423 K). At 0.25 V the contact temperature is not high enough to cause melting but may cause some amount of softening. At 0.5 V, there is more softening and at 1.0 V, the contact voltage is high enough to cause melting. At 2.0 V, boiling of the contact material is possible. When the hot switching voltage is increased up to 3.5 V, even more boiling and possibly ionization of metal vapor can occur.

It should be noted, with respect to the data presented in **Figure 3** and **Figure 4**, that 3 or more samples were tested for most test cases shown. Only for 0 V (cold switched), there were 2 samples tested for each polarity. For 1.0 and 2.0 V, the randomness in the direction of material transfer causes contacts tested under similar conditions to often look different which means the data shown is not typical to that particular case. For 0.25 V there is very little observable material transfer although some damage can be seen. For 0.5 V there were 4 samples tested for each condition (leading, trailing, both polarities) and all tests show the same material scatter. The material scatter is unlike what is observed for other voltages (except 3.5 V leading edge where it occurs 50-60% of the times) and is very repeatable. For 3.5 V, more than 15 tests have been performed for each condition and the polarity dependence is always obeyed.

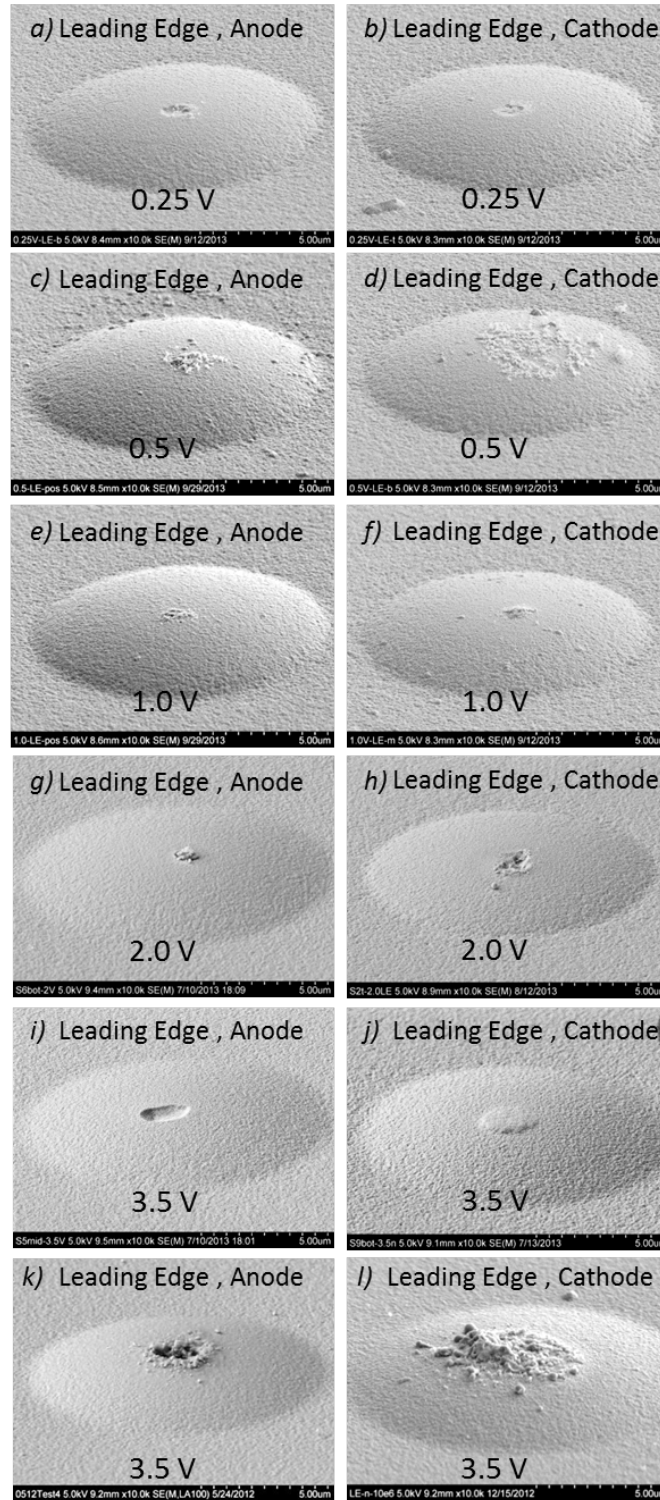


Figure 4. Leading edge hot switching contact bump damage at different voltages after 10^6 cycles. On-state current is 77.5 mA.

It is observed that more than 50% of the time, leading edge hot switching at 3.5 V leads to material scatter. However, unlike the 0.5 V results, the material transfer is polarity dependent. Also, the scattered

material shows formation of larger particles in the case of 3.5 V relative to 0.5 V, as shown in **Figure 5**. One reason for this could be that melting is expected at 3.5 V whereas for 0.5 V, only heating and softening of the Ru is expected.

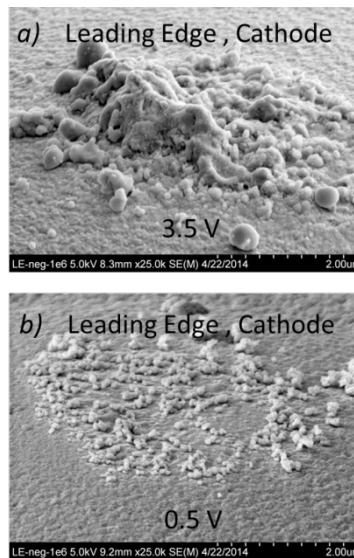


Figure 5. High resolution images of the contact bumps showing material scatter in leading edge hot switching when the contact bump is the cathode. a) 3.5 V, b) 0.5 V.

While hot switching always seems to lead to some amount of material transfer, it is important to note that the pits and mounds formed at either end of the contact may or may not be conformal as seen in **Figure 6**. In particular, for 0.5 V, when material scatter is significant, the damage areas seen on either side of the contact are not conformal. At higher voltages, the damage areas are generally conformal, with the exception of those leading edge hot switching tests that show significant scatter (similar in appearance to the scatter seen at 0.5V).

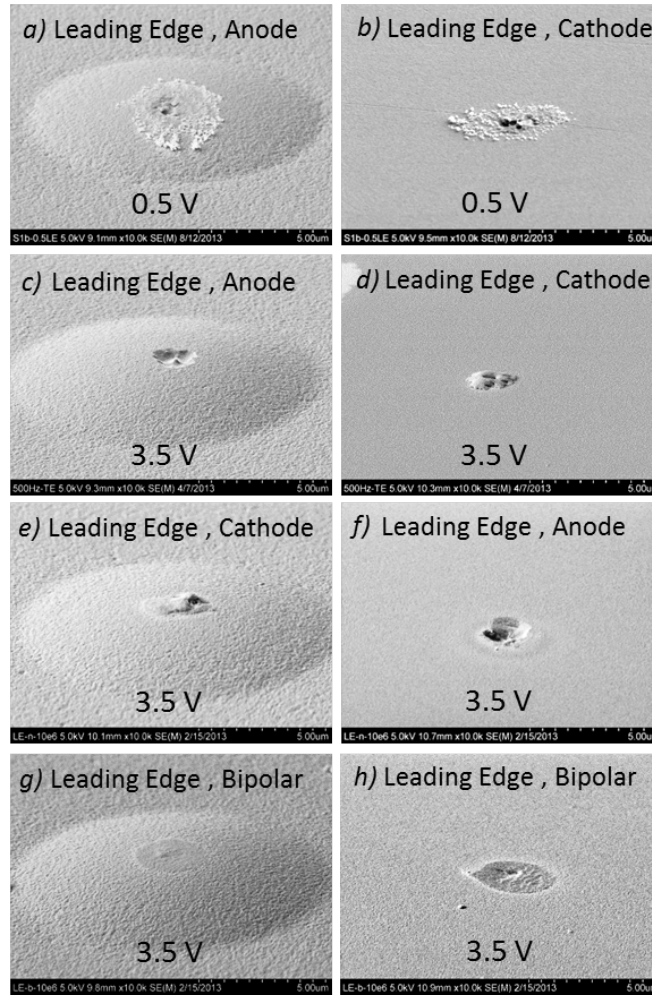


Figure 6. Non-conformal (a,b) and conformal (c-h) contact damage area at 0.5 V and 3.5 V hot switching voltages after 10^6 cycles. The on-state current was 77.5 mA. The left column shows the contact bumps while the right column shows the pillars.

3.3 Observation and investigation of pre-contact current – In [21] and [22], the presence of small currents of a fraction of a μA just before the contacts close was reported. The hot switching voltage that was applied across the contacts was 5 V. The currents were attributed to Fowler Nordheim tunneling. Similar currents were observed independently in the present work using a transimpedance amplifier (for higher bandwidth measurements) as well as a source-measure unit as reported in [36,37]. It was observed that, even at a hot switching voltage of 1 V (less than the work function of Ru), a pre-contact current was present, indicating that Fowler Nordheim tunneling alone is not responsible for this current.

In the course of the investigation of the pre-contact currents, it was discovered that they have a very small role to play in material transfer or hot switching contact damage under the conditions tested. It was observed that if a clean Ru contact, freshly deposited with the contact material, was tested within 1 day of the deposition process, the pre-contact current was not detected. The same was true if the test was conducted after the contact was cleaned with oxygen plasma as described in [20]. If the same contact was left in the AFM test system overnight, with the nitrogen flow off, then the following day the pre-contact current appeared again. **Figure 7** shows two graphs corresponding to a ‘dirty’ and a ‘clean’ contact. The graphs shown correspond to the same contact except that for the ‘dirty’ case, the contact was left in the AFM overnight.

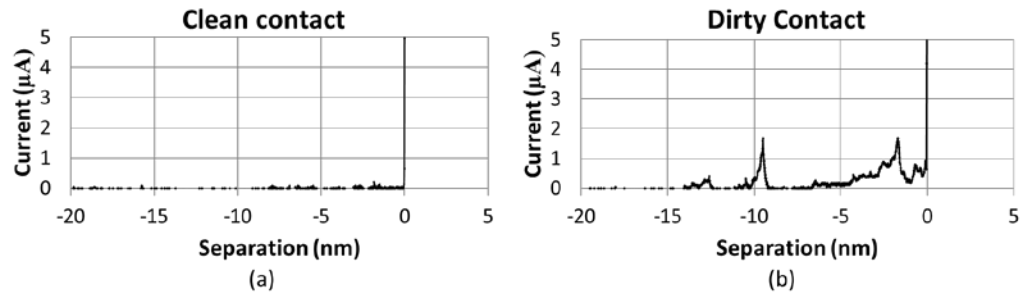


Figure 7. Pre-contact current in a) Dirty contact tested 2 days after deposition of contact material, b) Clean contact tested immediately after deposition of contact material

It should be noted here that material transfer observed at a hot switching voltage of 3.5 V takes place in Ru contacts with freshly deposited samples as well as samples tested a week after deposition. The fact that the absence of the pre-contact current does not lead to absence of material transfer suggests that the pre-contact current is not responsible for material transfer.

In addition, if the pre-contact current is part of the material transfer process, then such material transfer should be observed if the current is sustained at a small separation without allowing the contacts to close. To implement this scenario, several tests were conducted on contacts such that the pillar was allowed to approach the contact slowly until approximately 1 μA of current was observed. When current on the order of 1 μA was observed, the piezoactuator was paused and the contacts were held at a constant separation. The current was very unstable, typically varying from nearly zero to several μA . There was some amount of drift in the AFM piezo which typically caused the pre-contact current to change over a period of seconds. When the drift in the AFM piezo caused the contacts to become too close together or too far apart, the drift was compensated for by expanding or contracting the piezoactuator manually. **Figure 8** shows a typical 20 ms snapshot of the pre-contact current during one of these tests.

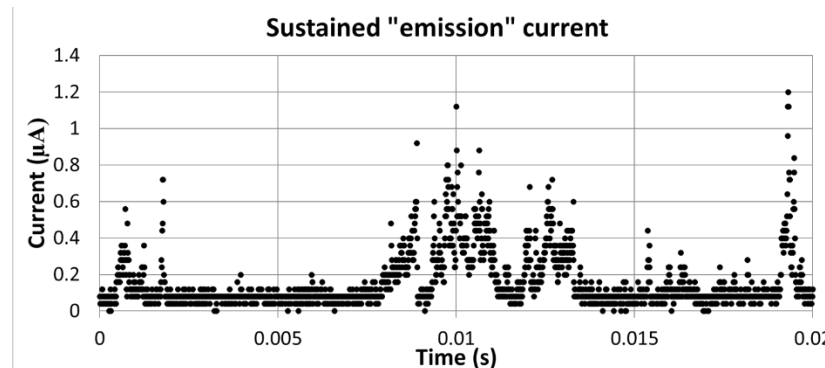


Figure 8. Pre-contact current allowed to sustain without closing the contacts (in a typical region)

After sustaining the current for around 40 minutes, the contacts were imaged using SEM. For contacts tested in this manner, there was no significant damage observed. **Figure 9** shows two contacts that were tested under these conditions and appeared completely undamaged.

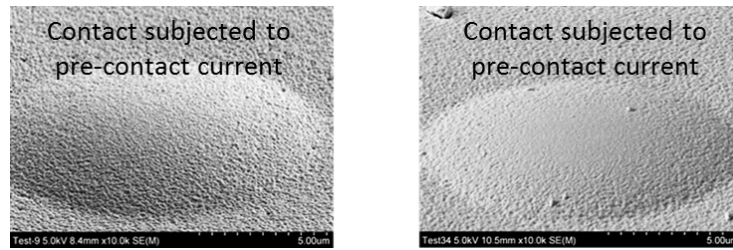


Figure 9. Undamaged contact bumps after sustained pre-contact current

These tests indicate that this pre-contact current is not related to the observed material transfer. One explanation for the observed current might be due to tunneling into or through the contamination layer formed. The insulating layer here is probably made out of carbonaceous compounds from the atmosphere adsorbed by the contact surface when the contact is kept in the AFM without nitrogen flowing for a period of time.

3.4 Analysis of the role of field emission and field evaporation in material transfer – While the pre-contact currents observed were shown not to have a role in material transfer, it is important to understand that field emission and field evaporation may still be significant at extremely small separations. Field emission can occur either by direct or Fowler Nordheim tunneling. Direct tunneling can occur when the applied voltage between anode and cathode is less than the work function of the metal. Fowler Nordheim tunneling can only occur when the applied voltage is greater than the work function of the metal.

For Ru, the work function is around 4.7 eV. Therefore, Fowler Nordheim tunneling cannot drive the material transfer at a 3.5 V hot switching voltage as observed in this work. If field emission is to be significant at this voltage, the mechanism has to be direct tunneling. Under this scenario, the separation between the contacts has to be small enough to allow direct tunneling. As explained later, this would imply that the electrodes must be separated by less than 0.5 nm for significant tunneling currents to flow. Under such circumstances, the picture of direct tunneling leading to material transfer will look somewhat as shown in **Figure 10** with the gap predicted to be on the order of 0.1-0.2 nm, or just 1 to 3 times the size of a Ru atom. **Figure 11** shows the rough schematic for two types of tunneling.

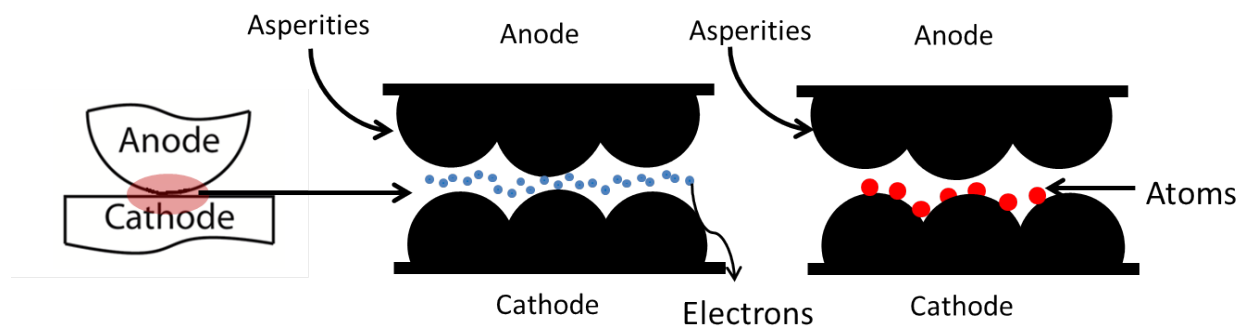


Figure 10. Proposed mechanism of direct tunneling leading to polarity dependent material transfer: Tunneling between asperities from cathode to anode followed by evaporation of contact material from anode to cathode resulting from the high local temperature.

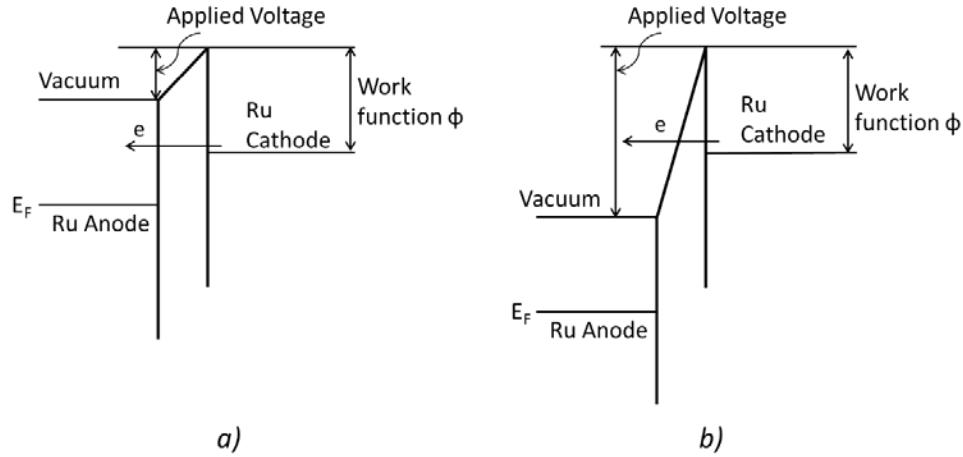


Figure 11. Fowler Nordheim and direct tunneling mechanisms for tunneling of electrons – a) Direct Tunneling from cathode to anode, b) Fowler-Nordheim Tunneling from cathode to vacuum

Given below are the equations for calculating the current density in the case of both types of tunneling as a function of several parameters.

$$J_{FN} = \frac{q^3 E^2}{16\pi^2 \left(\frac{h}{2\pi}\right) \phi} \exp \left[-\frac{4\sqrt{2m^*} \phi^{3/2}}{3\left(\frac{h}{2\pi}\right) qE} \right]$$

$$J_{DT} = \frac{q^2 E \sqrt{2mq\phi}}{4\pi \left(\frac{h}{2\pi}\right)^2} \exp \left[-\frac{2w\sqrt{2mq\phi}}{\left(\frac{h}{2\pi}\right)} \right]$$

In the above equations, J_{FN} and J_{DT} refer to the current density due to Fowler Nordheim emission and direct tunneling respectively. E is the electric field, m^* is the effective mass of the electrons, Φ is the work function and h is Planck's constant [38,39]. Using these equations, one can estimate the current that will be present. This is shown in **Figure 12**.

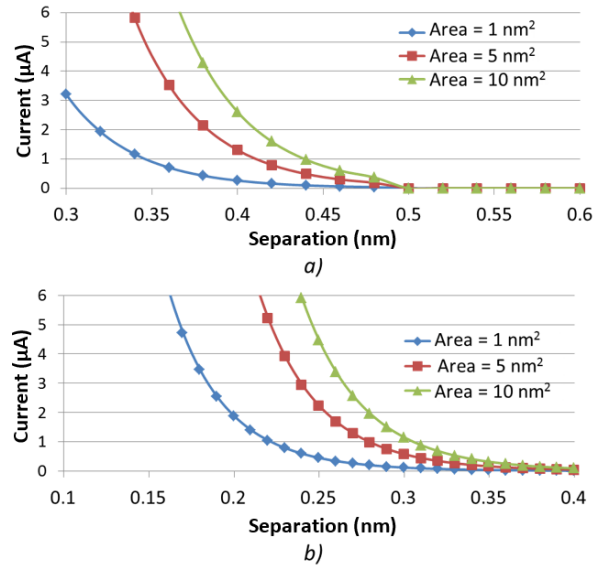


Figure 12. Tunneling current as a function of contact separation for a) Direct Tunneling and b) Fowler-Nordheim Tunneling

It is evident that a current of a few μA can be achieved when the contact area is 1 to 10 nm^2 . As an example, consider a separation of 0.34 nm between the contacts with an area of 1 nm^2 through which direct tunneling occurs. Under these circumstances, $1\text{ }\mu\text{A}$ current flows through tunneling. At a rate of $4400\text{ }\mu\text{m/s}$, the time required to close a separation of 0.3 nm is about 69 ns . Assuming (as a lower bound) $1\text{ }\mu\text{A}$ current, the number of electrons required to achieve this current flow in 50 ns is 3.125×10^5 . If each electron has 3.5 eV of energy, the total available energy would be $3.5 \times 1.6 \times 10^{-19} \times 3.125 \times 10^5 = 1.75 \times 10^{-13}\text{ J}$. Thus, as a lower bound, at least $1.75 \times 10^{-13}\text{ J}$ is available as the contact closes. Considering the thermal properties of Ru shown in **Table 1**, the amount of energy required to evaporate 500 nm^3 of Ru can be evaluated.

Table 1. Thermal properties of Ruthenium

Specific heat	0.024 kJ/mole-K
Melting temperature	2607 K
Specific heat of fusion	23.7 kJ/mole
Boiling temperature	4423 K
Specific heat of evaporation	567 kJ/mole

From these values, it was found that $5.72 \times 10^{-14}\text{ J}$ of energy is needed to evaporate 500 nm^3 of Ru. However, this calculation does not account for any source of inefficiency in energy transfer or any energy lost to the surrounding environment – both would be present in any real system; thus, this estimate is a lower limit on the energy required to vaporize 500 nm^3 of ruthenium.

Field evaporation, shown in **Figure 13**, is another candidate for the observed material transfer. Although such a phenomenon could well give rise to some material transfer for microcontacts, the minimum threshold electric field required for field evaporation in Ru is 42 V/nm . Assuming no field enhancement, this would imply about 0.8 nm separation between the contacts in order to get field evaporation when the voltage between the contacts is 3.5 V . It is noted that the presence of a sharp asperity on one surface can lead to some amount of field enhancement which might make it possible to get field evaporation at larger separations. However at very small separations, such enhancement becomes less likely.

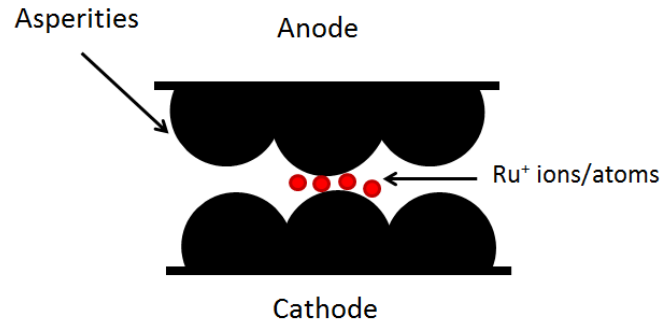


Figure 13. Field evaporation between contacts with small separation: Positive Ru ions are pulled from anode on to the cathode leading to material transfer.

Although field enhancement due to pointed asperities becomes unlikely at small separations, the threshold voltage required for field evaporation is reduced as the separation between electrodes reaches sub-nm levels [40]. As the separation becomes smaller, the anode and cathode interaction profiles start overlapping which leads to a double-well structure. This results in a reduction of the binding energy that an atom needs to overcome in order to move from one electrode to another. This can be thought of as the field evaporation equivalent of direct tunneling in electrons where a small contact separation can lead to electrons tunneling even at very low potentials. The electric field required for evaporation at this stage will drop by 50% if the separation between the electrodes is less than 4 Å [40]. For a voltage of 3.5 V, the separation required for field evaporation can be estimated to be around 1.5 Å.

3.5 Evidence of leading edge hot switching damage being a low current phenomenon – For leading edge hot switching, the capacitances of the circuit and device play a role in determining the current at the point of contact. In this test setup, a parallel-plate capacitor model considering the SiO₂ isolation layer between the device and handle sides of the chip predicts a capacitance of approximately 35 pF. In order to analyze the effect of this added capacitance, a SPICE model was used. With a switching frequency of 500 Hz, test data captured during the experiments showed the contact resistance dropping from infinity to around 1 ohm within 10 μs. The SPICE model was set up accordingly as shown in **Figure 14**.

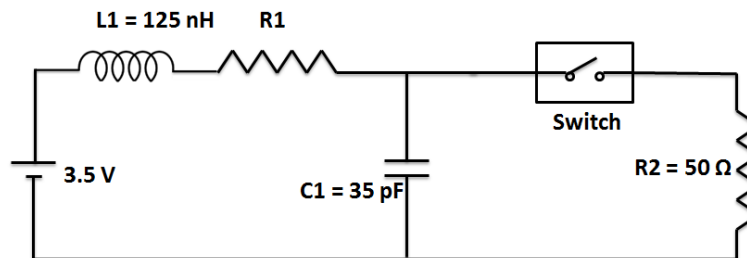


Figure 14. Equivalent circuit for the test setup

R1 is the external series resistor that was varied in order to analyze its effect on the circuit response. L1 is the inductance in the system due to the interconnecting wires, C1 is the parasitic capacitance of the device (described above), and R2 is a 50 Ω termination. **Figure 15** shows the current as a function of time using various values of R1. It is concluded from the SPICE model that the current overshoot is not significant for an external series resistance of less than about 5 kΩ with an applied voltage of 3.5 V. For resistances above 5 kΩ, current overshoot is observed which becomes large compared with the steady state current for resistances above 20 kΩ. For resistances above 1 MΩ, the current overshoot was larger on the first cycle because the capacitance did not have enough time to charge up between cycles. Experimentally, contact damage was studied with series resistances (R1+R2) from 50

Ω to $10\text{ M}\Omega$. The SEM images in **Figure 15**, correspond to contact damage at different values of external resistance are shown. It is clear that up to a resistance of $1\text{ M}\Omega$, the contact damage is significant. The micrographs also suggest that the current/voltage that causes contact damage is higher than what exists with a $10\text{ M}\Omega$ resistor since Figure 15(f) does not show significant damage.

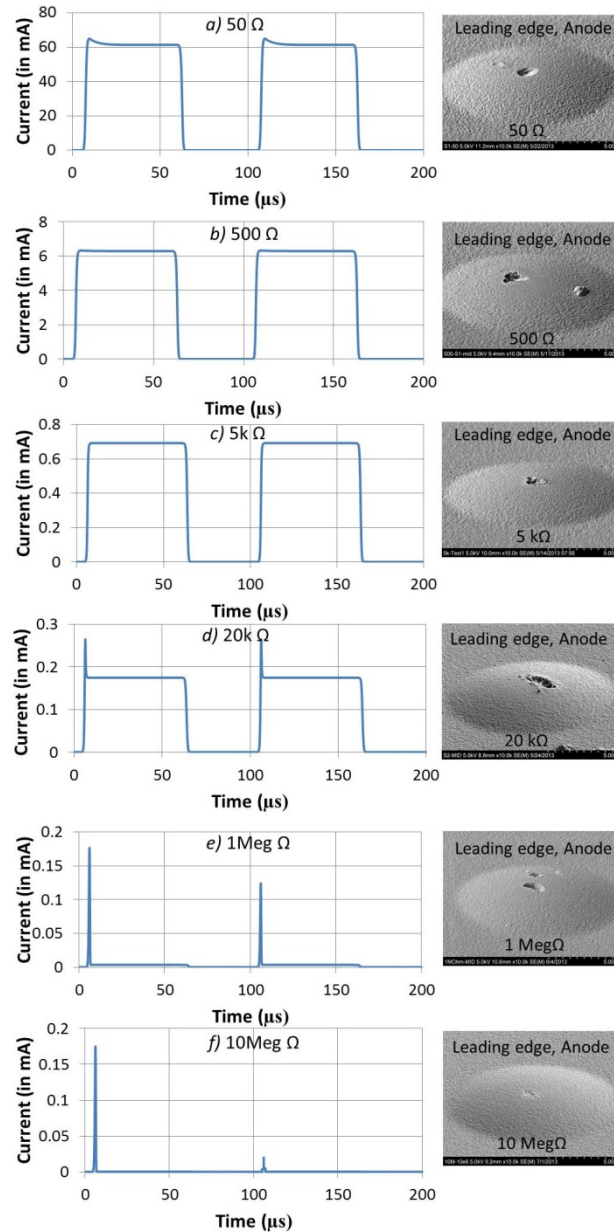


Figure 15. Modeled transient current response with images of contact bumps (inset) after 10^6 cycles of leading edge hot switching with an external resistance of a) $50\ \Omega$, b) $500\ \Omega$, c) $5\text{ k}\Omega$, d) $20\text{ k}\Omega$, e) $1\text{ M}\Omega$ and f) $10\text{ M}\Omega$. Note that for 1 and $10\text{ M}\Omega$ the second current spike is smaller than the first since the capacitance cannot charge up to its full value when RC constant becomes comparable to the time between subsequent contacts.

Effectively, therefore, for resistances less than about 10 k Ω , the current during the switching event is determined by the series resistance and is affected little by the capacitance. For resistances from 20 k Ω to 1 M Ω , it was found that the capacitance sets the peak current at about 0.15 mA. For resistances greater than 1 M Ω , the peak current decreases with increasing resistance (although it is important to note that this last transition depends on the cycling frequency). Given the contact damage observed for higher resistance values (20k Ω and 1M Ω), we conclude that the current required for the observed material transfer is less than 0.15 mA. In most RF circuits, considering a characteristic impedance of 50 Ω , the capacitance should not have an effect on the contact damage.

3.6 Leading and trailing edge hot switching with high external resistance – We previously reported that both leading and trailing edge hot switching at 3.5 V result in quantitatively the same amount of material transfer irrespective of whether the contact bump is the anode or the cathode [20]. This result suggests the presence of similar mechanisms at both edges of a hot switching cycle. However, as earlier shown in **Figure 4**, leading edge hot switching sometimes results in contact damage with widely scattered debris, while trailing edge hot switching does not.

In addition, the damage from leading and trailing edge hot switching tests were found to be quantitatively different when tested under certain conditions. Contacts were tested with a series resistance of 5 k Ω at a voltage of 3.5 V for 10⁶ cycles. As shown in **Figure 16**, leading edge hot switching causes more damage than trailing edge hot switching under these conditions. The images shown correspond to two tests conducted for leading and trailing edge hot switching with 5 k Ω resistors.

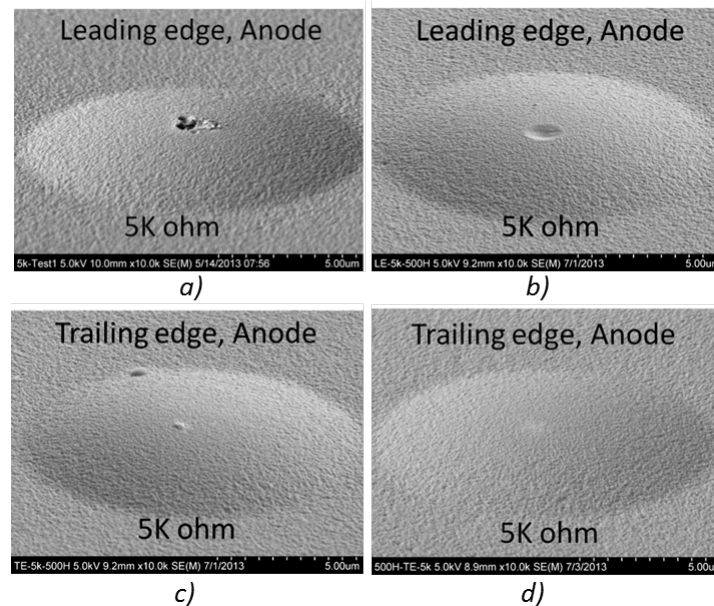


Figure 16. Comparison of contact damage at 3.5 V and 5k Ω external resistance between leading and trailing edge hot switching after 10⁶ cycles. All images shown are of contact bumps.

This difference in damage can be attributed to the presence of the capacitance in the circuit. With a capacitance of 35 pF and a resistance 5 k Ω , the voltage across the capacitance takes time to build up as the contact starts separating effectively reducing the voltage across the contact which leads to less damage.

3.7 Slow approach and separation of contacts – Tests were performed to study the effect of slow approach and separation of contacts at hot switching voltages of 3.5 V and 5 V. The tests were run for 40-

45 minutes at an approach/separation rate of 8.8 nm/s. Figures 17 to 20 show the results that emerged from these tests.

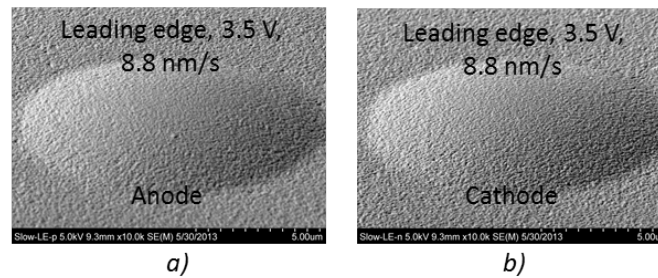


Figure 17. Leading edge hot switching tests at 3.5 V hot switching voltage, 50 Ω resistor, with contacts approached at 8.8 nm/s: a) Contact bump is anode, b) Contact bump is cathode

Figure 17 represents tests where a hot switching voltage was applied only at the leading edge. Here, the hot switching voltage applied is 3.5 V with an external resistance of 50 Ω . With an approach rate of 8.8 nm/s, 50 switching cycles were performed. On examining the contacts after cycling, no observable damage to these contacts was detected either for the case where the contact bump was the anode, or when it was the cathode. By reducing the ramping rate by a factor of 500,000 and decreasing the number of cycles by a factor of 25,000, the time the contacts spend in close proximity should ideally increase by a factor of 20 relative to the standard test. The material transfer under these conditions is insignificant which points toward a mechanism that depends on the number of switching cycles rather than the time spent in close proximity. One explanation for this behavior is that the material transfer mechanism occurs when the separation is close enough for electrostatic force to pull the contacts together, thus making the mechanism independent of the approach rate.

Figure 18 and **Figure 19** represent tests where a hot switching voltage was applied only at the trailing edge. **Figure 18** corresponds otherwise to the same conditions as **Figure 17** i.e. a hot switching voltage of 3.5 V and a ramp rate of 8.8 nm/s. **Figure 19**, on the other hand, corresponds to an applied voltage of 5 V. The contacts were cycled 50 times for all the tests shown.

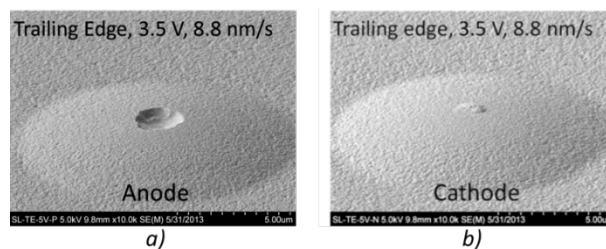


Figure 18. Trailing edge hot switching tests at 3.5 V hot switching voltage, 50 Ω resistor, with contacts separated at 8.8 nm/s: a) Contact bump is anode, b) Contact bump is cathode

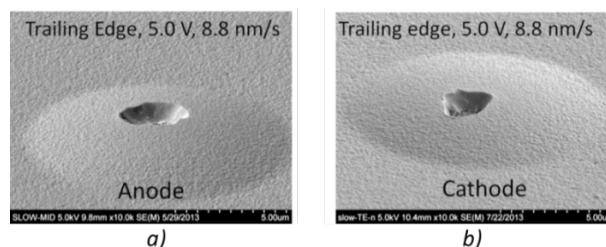


Figure 19. Trailing edge hot switching tests at 3.5 V hot switching voltage, 50 Ω resistor, with contacts separated at 8.8 nm/s: a) Contact bump is anode, b) Contact bump is cathode

From **Figure 18** and **Figure 19**, it can be concluded that for trailing edge hot switching, the duration of weak contact or close proximity plays a role in the amount of material transfer. We observe that within just 50 cycles, the contact damage is as significant as that seen after 1 million cycles with the usual switching rate of 4400 $\mu\text{m/s}$.

It is also observed that the material transferred for slow trailing edge hot switching is polarity dependent when the voltage applied is 3.5 V. However, between 3.5 V and 5.0 V there is a change in the dominant mechanism for material transfer. At 5.0 V, irrespective of the polarity of the material transfer, material is always transferred away from the contact bump. Also, at 3.5 V, the material transferred away from the contact bump when the contact bump is the anode appears to be greater than the material transferred on to the bump when it is the cathode. This seems to suggest that there are two mechanisms occurring simultaneously which either reinforce or oppose each other. One mechanism is likely related to the temperature difference between the contact and the pillar purely on account of the thermal conductivity difference. The other is a polarity dependent mechanism.

Yet another set of experiments for trailing edge hot switching was conducted where the contacts were not allowed to come apart. The current through the contact decreased with an increase in contact resistance but was then held at 75-80 mA for the entire test. Essentially therefore, any mechanism that depends upon an electric field between open contacts is taken out of the equation when the contacts are tested in this manner. At 80 mA of current, the contact voltage is approximately 1 V which is high enough for melting but may be just less than boiling. This possibly leads to formation of a molten bridge. The contacts were kept at this melting voltage point for about 40 minutes. The results of these tests are shown below in **Figure 20**.

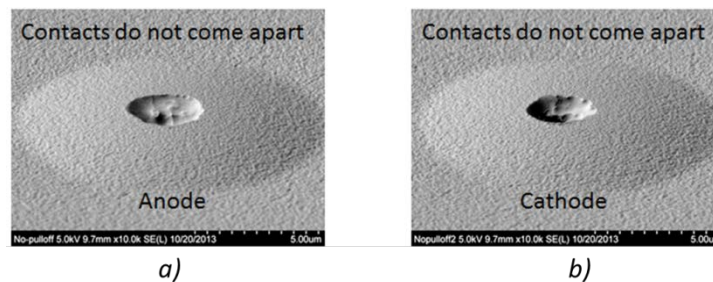


Figure 20. Slow tests at an approach/separation rate of 8.8 nm/s, at a voltage of 5V and external resistance of with contacts not being allowed to come apart: a) Contact bump is anode, b) Contact bump is cathode

The results from **Figure 20** strongly suggest that a polarity independent material transfer mechanism is present at the trailing edge and is probably the same as that observed in **Figure 19** where the contacts were allowed to come apart. This mechanism results in transfer of material from the force measurement structure to the pillar.

3.8 Bipolar and high frequency AC hot switching tests – In **Figure 21**, material transfer is shown for the contact bump as anode, the contact bump as cathode and the contact bump alternating between cathode and anode on each switching cycle (bipolar). Tests were conducted for both leading and trailing edge hot switching at 3.5 V, 500 Hz, 10^6 cycles, and 50Ω series resistance. As shown here, we find that the material transfer is always from anode to cathode for unipolar hot switching. For bipolar hot switching the material transfer in the two directions nearly cancels, resulting in far less net material transfer for the same number of cycles. Nevertheless, we observe that the area modified by contact expands as the number of cycles increases, the contact bump and the pillar become nearly conformal in the modified area, and the modified area is roughly comparable in area to the modified area on the unipolar contacts. Contact pairs illustrating these effects were also shown earlier in **Figure 5**.

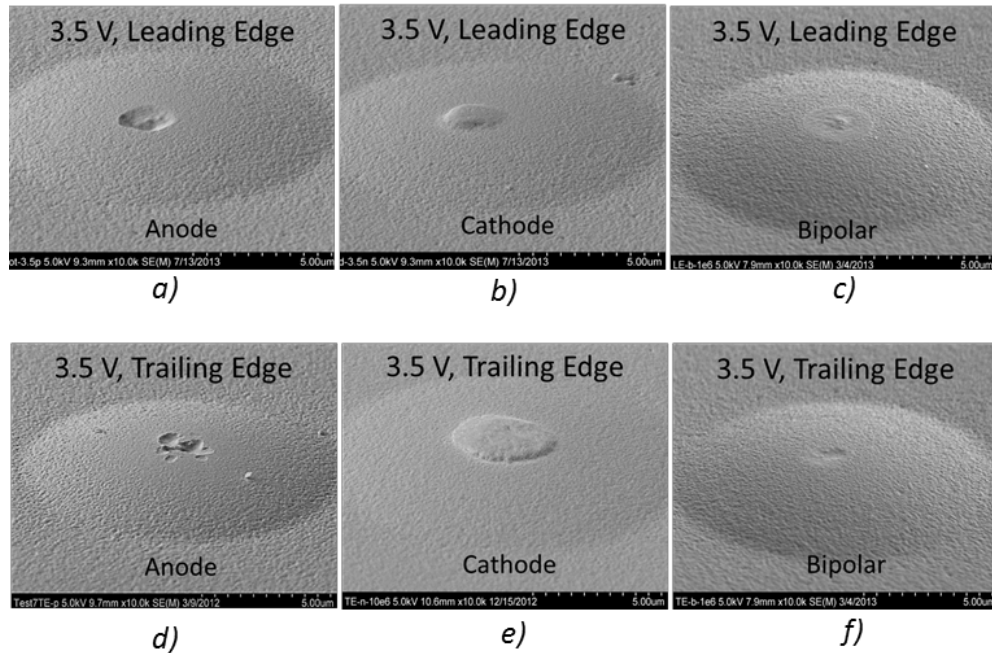


Figure 21. Leading and trailing edge hot switching tests for comparing bipolar to unipolar contact damage for 10^6 cycles with 3.5 V hot switching voltage and 77.5 mA on-state current – a) Leading edge hot switching with contact bump as anode, b) Leading edge hot switching with contact bump as cathode, c) Leading edge bipolar hot switching, d) Trailing edge hot switching with contact bump as anode, e) Trailing edge hot switching with contact bump as cathode, f) Trailing edge bipolar hot switching.

Subsequently, much longer tests were conducted with bipolar hot switching to see if a net transfer of material would occur despite the near cancellation because of the bipolar testing. Two tests were conducted up to 4.0×10^7 cycles (one each for leading and trailing edge) and one test up to 1.2×10^8 cycles was performed and the contacts examined. **Figure 22** shows the images of the contact bumps after the tests were concluded. **Figure 23** shows the contact resistance and adhesion in the contact over the course of the test that lasted 120 million cycles. The corresponding image of the contact is shown in Figure 22(c). It is important to note here that adhesion, considered an important damage mechanism during hot switching, remains low throughout the course of this test (the pull-off force is less than 75 μN for contacts with a 400 μN contact force). Also the contact resistance remains low throughout the test, suggesting that these contacts may be reliable for more than 10^8 cycles, even with hot switching at 3.5 V and 78 mA.

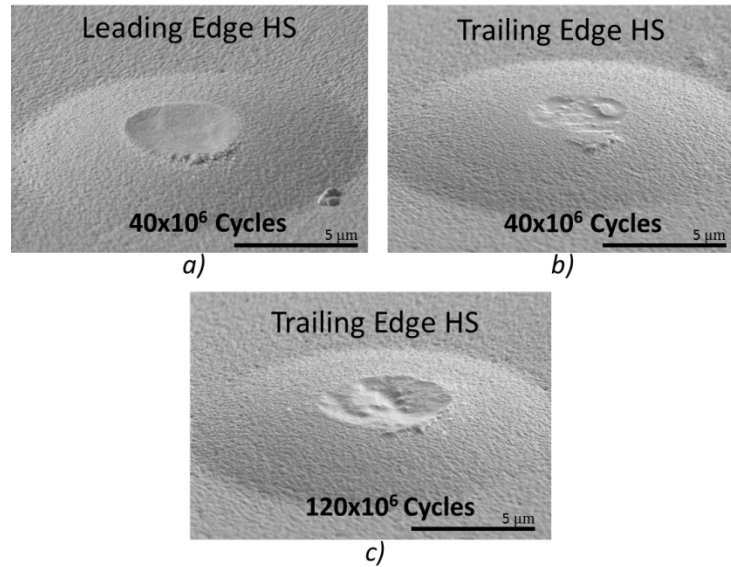


Figure 22. Contact bumps after bipolar hot switching with 3.5 V hot switching voltage and 77.5 mA on-state current – a) Leading edge, b) Trailing edge, c) Trailing edge

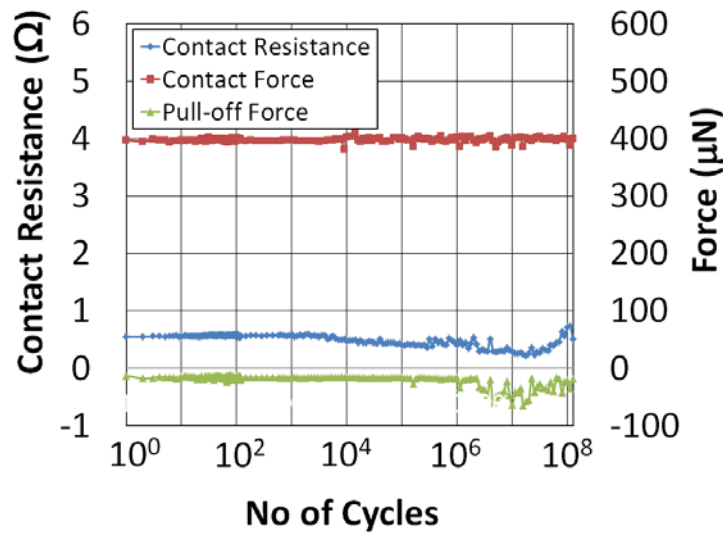


Figure 23. Contact resistance, pull-off force and contact force vs number of cycles for a long term bipolar hot switching test.

As seen in **Figure 21** and **Figure 22**, the net amount of material transfer in the bipolar case is much less than for dc hot switching. This is not surprising since it is expected that material will transfer from the anode to the cathode, which for the bipolar case means that material will transfer back and forth between the two electrodes. As shown in [20], the magnitude of material transfer is approximately independent of polarity of the force sensor and pillar, implying that the amount of material transferred in the two directions will be nearly equal.

Also shown in **Figure 22** is that there is a slow net transfer of material in the bipolar case, from the force sensor to the pillar. The observation that the volume of material transferred is independent of the polarity of the force sensor and pillar suggests that a mechanism, different from the one responsible for the anode to cathode transfer of material, exists in the bipolar case. It is possible that any melted or evaporated asperity on either of the contacts might have a bias toward transferring material to the cooler

side, resulting in material transfer from bump to pillar as observed in the bipolar experiments. On the other hand, the net transfer is small, so it could be a result of small differences between the operations of the polarity-dependent mechanism in the two directions.

Figure 24 shows contact damage when tests were conducted with an AC hot switching voltage applied to the contact from a function generator with a source impedance of 50Ω . The amplitude of the applied voltage was 10 V p-p or 3.5V rms. The frequency of the applied voltage was swept from 18 to 20 MHz. This corresponds to approximately 0.5 cycles of the sinusoidal voltage in the time it takes the contacts to approach or separate by 1 \AA . This implies that during the time for which contact separation is in the regime where field emission and field evaporation are likely to be significant, the hot switching voltage would vary from 0 to 5 V. The contacts in these tests were cycled up to 10^6 cycles. These results indicate that AC hot switching damage at a moderately high frequency is very similar to bipolar hot switching under similar conditions and after similar number of cycles.

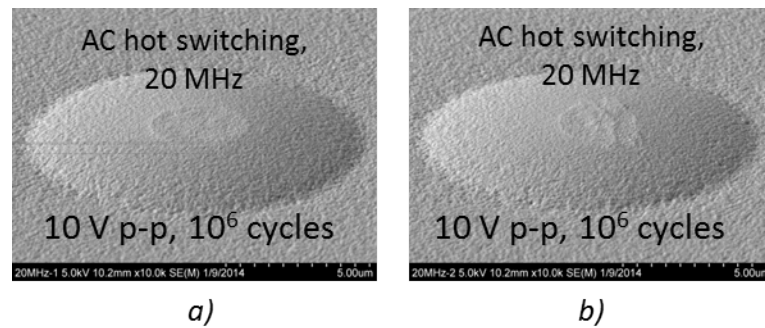


Figure 24. Contact bumps after 10^6 cycles with a 10 V p-p (3.5 V rms) AC voltage at 18 – 20 MHz

3.9 Thermal effects and electromigration – In the Maxwell contact regime, when the contact is significantly larger than the mean free path of electrons, the temperature of the contact spot varies with the contact voltage using the relationship given in [29] and mentioned in Section 3.2. Using this relationship, the melting voltage of Ruthenium comes to around 0.8 V. Furthermore, if the Lorentz's constant (product of thermal conductivity and electrical resistivity of the contact material) is assumed unchanged in the vapor state, the boiling voltage of Ru will be around 1.35 V.

Melting can occur for both leading and trailing edge hot switching. However, for leading edge hot switching, melting will lead to contacts sinking into each other thereby increasing the contact area which leads to lower contact resistance and lower voltage across the contact, and ultimately solidification of any melted area. At the trailing edge, we can have one of two outcomes. One possibility is that the contacts can pull apart suddenly and completely after initial adhesion. A second possibility is that as the contact area gets smaller the contact voltage approaches the melting voltage. At this stage, a molten metal bridge will be formed while the contacts continue to pull apart. This may cause the temperature of the bridge to continue to increase beyond its melting point. If the temperature is high enough, the molten bridge can evaporate and ionize leading to positively charged ions which are attracted toward the cathode, resulting in material transfer from the anode on to the cathode.

For ionization of a vapor of Ru metal, a high temperature is required. The relationship between the ionization fraction of a volume of vapor and its temperature is given by the Saha equation [41,42]

$$\log_{10} \frac{n_i^2}{n} = -5400 \frac{V_i}{T} + \frac{3}{2} \ln T + 15.85$$

Here n_i and n correspond to the number density of the ions and the neutral atoms respectively. V_i is the ionization potential which is 7.36 for Ru and T is the absolute temperature. **Figure 25** shows the approximate relationship between ionization fraction and temperature of the Ru vapor. The number

density of ions and neutral atoms combined can be calculated as $n = \frac{N_A}{M} \rho$ where N_A is Avogadro's number, M is the molar mass and ρ is the mass density of Ru. As an upper bound on density the density of liquid Ru is used, giving an ionization percentage of 30% at approximately 5700 K. As a lower bound on density, we use a density corresponding to an ideal gas at 1 atmosphere. This gives a number density between $7.3 \times 10^{18} \text{ cm}^{-3}$ to $1.8 \times 10^{18} \text{ cm}^{-3}$ as temperature is varied from 1000 to 4000 K. An ionization percentage 30% is reached at 3700 K. These results indicate that near the boiling point (4423 K), Ru is likely to be in an ionized state causing material to be pulled toward the cathode.

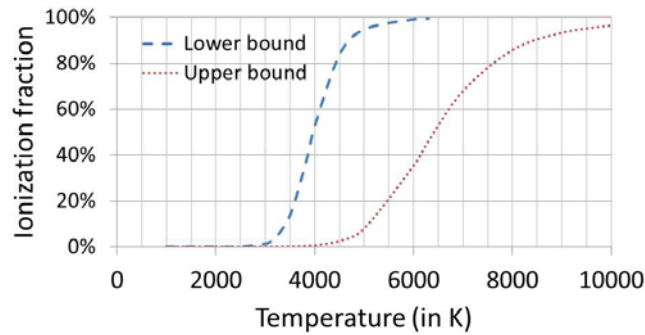


Figure 25. Upper and lower bounds for temperature required for ionization

Electromigration can also result in material transfer. Electromigration refers to mass transport in a conductor that occurs as a result of high current densities [28,43]. At current densities above 10^4 A/mm^2 , electromigration can become significant. If we consider a current of 75 mA as the contacts begin to open, typical for our testing, then the radius of the bridge needs to be $0.75 \text{ }\mu\text{m}$ to achieve this current density. For a microcontact, the radius of the contact spot, just before opening, is an order of magnitude (or more) smaller than this, giving a much higher current density and an increased amount of electromigration occurring.

Electromigration can lead to material transport either with or against the electric field. The electric field in the metal pulls electrons towards the cathode, while the ions are pulled towards the anode. However, the energy transferred to the ions from collision with electrons can result in the ions drifting towards the cathode together with the electrons. Thus, there are two opposing forces acting on the ions. The net drift velocity of the ions due to electromigration is given in literature by the following equation [28,43]:

$$V = JeZ^* \rho D / KT$$

Here, V is the velocity of ion transport; Z^*e is the effective charge in the ion taking into account electrostatic force due to applied electric field, as well as the influence of the electrons; ρ is the resistivity of the contact material, D is the diffusion coefficient of the ions, K is Boltzmann's constant and T is the absolute temperature of the contact spot. Usually, electromigration in metals occurs in the direction of flow of electrons i.e. cathode to anode which implies $Z^* < 0$. In a liquid, however, since the ions have additional thermal energy, they may be prone to move towards the cathode. Anode to cathode material transfer has been reported in Al, Ag, In and other metals, particularly in the molten state [29,44,45].

Asymmetry in the thermal conductivity between the anode and the cathode can lead to material transfer. At the time of contact opening, if a metal bridge is formed it will eventually break at its hottest point since the area around that point is likely to evaporate first. In our contacts, this hottest point will tend to be biased away from the pillar, which is the better heat sink on account of its higher thermal conductivity [46]. As a result of this, there will be asymmetric transfer of material towards the pillar irrespective of the polarity of the applied voltage. This effect, therefore, will be polarity independent and

will always lead to material transfer away from the contact bump. It is likely that the material transfer observed with bipolar hot switching and slow separation tests are due to this mechanism.

The Thomson effect can also lead to asymmetric heating and material transfer. In a metal bridge, a temperature gradient will occur as a result of the voltage across the contact and the flow of current [29,47]. The temperature gradient may be from anode to cathode or the other way around depending on the sign of the Thomson coefficient. A positive Thomson coefficient leads to the cathode being hotter. This is exhibited in metals such as Cu and Ag. A negative Thomson effect, exhibited in Pt, Ni and Bi, leads to the anode being hotter [48]. However, when Pt was investigated, it was found that depending on its state (solid or liquid), its Thomson coefficient can change signs [29]. In the event of a molten bridge being formed while the contacts start to separate, the molten bridge will break at the point of the highest temperature and therefore will lead to material being transferred from the hotter to the cooler electrode. For the polarity dependent material transfer observed during trailing edge hot switching, the Thomson effect is a possible mechanism causing it.

3.10 Summary of mechanisms – From the results and the preceding discussion, it can be concluded that several mechanisms contribute to hot switching damage in microswitch contacts. For example, the nature of material movement/transfer changes from 0.5 V to 2 V to 3.5 V in a predictable way that is certainly due to different mechanisms being active. In addition, some types of observed damage have several candidate mechanisms. To summarize, some of the likely mechanisms are – a) Mechanical transfer through softening/adhesion/cold-welding as observed in low voltage hot switching; b) Mechanical transfer after melting as in leading edge hot switching with voltages greater than 1V; c) Field evaporation; c) Field emission leading to heating, melting and evaporation; d) Electromigration; e) Ionization of metal vapor; f) Formation of a metal bridge where the Thomson effect and thermal asymmetry can cause the hottest point of the bridge to be biased towards one of the electrodes.

Mechanical transfer through adhesion/cold-welding appears to manifest itself particularly during low voltage hot switching. At 0.25 and 0.5 V, when the contact temperature is not high enough to cause melting, heating and softening of the contact spot may lead to enhanced contact adhesion followed by material transfer while opening. For example, at 0.5 V, significant material scatter after many cycles of leading or trailing edge hot switching is observed. At 1-2 V, when contact melting is predicted, much less material scatter is observed, indicating that the material transfer mechanism is different when the contact melts. Up to 2.0 V, the observed material transfer is polarity independent. At 3.5 V, however, the material always transfers from the anode to the cathode. For leading edge hot switching at 3.5 V, significant material scatter is sometimes observed which may be due to a similar mechanism that leads to material scatter for 0.5 V, but with adhesion cause by melting (welding) at the leading edge in addition to softening and adhesion as in the lower voltage contact. For trailing edge hot switching, material scatter is never observed at 3.5 V, possibly because softening and melting only occur as the contact is in the final stages of pulling apart.

Field emission and field evaporation are both candidates for polarity dependent material transfer. For field emission, a separation on the order of a few Å is necessary in order to achieve the necessary current of approximately 1 μA. Material transfer due to this mechanism will be from anode to cathode. Field evaporation might also become important at such small separations leading to material transfer, also from anode to cathode. At small separations (less than 1 nm), the atoms can essentially tunnel from one surface to another at electric fields which can be 50% lower than the threshold value required for field evaporation at large separations. This phenomenon leading to material transfer at low voltages is also observed in STM tips when the sample is held close to it [49,50,51]. In [40], field evaporation has been suggested as a likely mechanism along with surface diffusion caused by heating of the apex of the STM tip.

Electromigration and the Thomson effect are two other polarity dependent mechanisms that can lead to material transfer when the contact is small and the voltage and current density are large. In the case of electromigration, the direction of movement of atoms will depend upon the direction of the net force experienced by them due to a) electrostatic force due to the electric field and b) collision of

electrons. For the Thomson effect, the direction of movement of atoms will depend upon the Thomson coefficient which can be positive or negative. In some cases, the Thomson coefficient can even change signs as a material gets converted from its solid to its liquid state.

Another mechanism explored which can lead to material transfer is formation of a metal vapor and subsequent ionization. This can occur at the leading edge or the trailing edge. At the leading edge, when there is initial contact between the highest asperities, the contact voltage can be high enough to cause boiling of the contact material. The metal vapor so formed can have high enough temperature to be ionized. At the trailing edge, a possible formation of metal vapor can be due to initial formation of a metal bridge which then evaporates when the voltage across it reaches the boiling voltage of the contact material. This metal vapor can also be ionized leading to positive ions being attracted towards the cathode.

The two contact surfaces often become conformal after many contact cycles. This might be explained by the combination of very short-range material transfer mechanisms (as described earlier), combined with some spreading out of material as the transfer occurs. Whatever the mechanism, a process of this type would construct conformal bumps and pits in the two electrodes, for dc hot switching, because it would spread out areas that touched sooner than other areas. The process would also cause the conformal area to spread as the number of cycles increases, as observed in dc, bipolar, and ac hot switching. On the other hand, when we see a large amount of material scatter, the two sides do not appear to be conformal, suggesting a different process, possibly one that involves pulling material out of one side of the contact or the other after adhesion (promoted by cold or hot welding).

Although it is impossible to specify the exact mix of active mechanisms during the course of a switching cycle in a typical MEMS switch, this work demonstrates that hot switching is a complex phenomenon in which polarity-dependent mechanisms are active at voltages above 3.5 V and polarity-independent mechanisms are active at voltages below 2.0 V. In addition, geometry-dependent (probably temperature-dependent) mechanisms are active at the same time, and dominate under some test conditions. Bipolar and ac hot switching act to largely cancel the polarity-dependent mechanisms allowing the geometry-dependent mechanisms to be observed. At the same time, this cancellation greatly prolongs the contact lifetime.

Although not directly investigated, the damage mechanisms discussed in this paper give some insight into how material transfer will be affected by the choice of contact materials. Other than field evaporation, all the other damage mechanisms tell us that materials with a higher melting or boiling point will tend to have less material transfer and presumably better reliability for hot switching. If field emission contributes to material transfer, the work function of the contact material will be another important property to be considered. For field evaporation related material transfer, the threshold voltage/field required for the atoms to be emitted would be the critical parameter.

4. Conclusions

This paper describes the complexity of hot switching in MEMS switch contacts. Hot switching tests at different voltages demonstrate the presence of at least four different regimes of contact damage. The complexity is further demonstrated by the presence of material scatter during leading edge hot switching at 3.5 V which is absent for trailing edge hot switching. The pits and mounds formed on the contacts during material transfer are usually conformal unless large amounts material scatter are observed. At a slow separation rate, the observed contact damage has different characteristics compared with the usual contact separation rate of 4400 $\mu\text{m/s}$. When contacts are separated extremely slowly, at a rate of 8 nm/s, an applied hot switching voltage of 3.5 V causes the polarity dependent mechanism to play a greater role than the polarity independent mechanism (possibly thermal). At 5 V, however, the polarity independent mechanism is dominant and leads to material transfer away from the contact bump.

It is also noted that pre-contact currents, observed in ‘dirty’ contacts do not cause material transfer. The observed pre-contact current is very likely caused by a contacts being separated through a layer of contamination and is absent when a freshly deposited or cleaned contacts are tested.

Certain damage mechanisms operate when the contacts are separated but in very close proximity (on the order to several Å), field emission and field evaporation being two such mechanisms. Other mechanisms operate when the contacts are barely touching or are connected through a molten metal bridge (Joule heating leading to evaporation and ionization, the Thomson effect and electromigration).

It was also observed that bipolar and AC hot switching result in much less contact damage compared with unipolar dc hot switching. With bipolar hot switching the contact resistance remained low, varying between 0.6 Ω and 0.8 Ω with contact resistance first going down and then starting to go up after about 20 million cycles. Adhesion did not increase significantly during the period, reaching a maximum of 75-80 μN with a contact force of 400 μN .

Acknowledgments

This work was supported by the Defense Advanced Research Projects Agency (DARPA) N/MEMS S&T Fundamentals program under grant no. N66001-10-1-4006 issued by the Space and Naval Warfare Systems Center Pacific (SPAWAR) as well as the membership of the RF MEMS Center at UCSD.

References

- 1 M. Daneshmand, R.R Mansour (2011), “RF MEMS Satellite Switch Matrices”, *IEEE Microwave Magazine* 12(5), pp 92-109.
- 2 Chris Keimel, Glenn Claydon, Bo Li, John Park and Marcelo E. Valdes (2011), “Micro-Electromechanical-System (MEMS) Based Switches For Power Applications”, 2011 IEEE Industrial and Commercial Power Systems Technical Conference (I&CPS), 1-5 May 2011 pp.1,8.
- 3 Hei Kam, Tsu-Jae King Liu, Vladimir Stojanović, Dejan Markovic, Elad Alon, “Design, Optimization, and Scaling of MEM Relays for Ultra-Low-Power Digital Logic,” *IEEE Transactions on Electron Devices*, vol.58, no.1, pp.236,250, Jan. 2011.
- 4 Paul M. Zavracky, N. E. McGruer, Richard H. Morrison, David Potter (1999), “Microswitches and Microrelays With A View Toward Microwave Applications”, *International Journal of RF and Microwave Computer-Aided Engineering* 9(4), pp 338-347.
- 5 Gabriel M. Rebeiz, “RF MEMS: Theory, Design and Technology”, John Wiley & Sons, Hoboken, NJ, 2003.
- 6 J. Maciel, S. Majumder, R. Morrison and J. Lampen (2004), “Lifetime characteristics of ohmic MEMS switches”, *Proc. SPIE*, vol. 5343, pp. 9-14, 2004.
- 7 S. Day, T. Christenson (2013), “A High Aspect Ratio Microfabricated Reed Switch Capable of Hot Switching,” 2013 IEEE 59th Holm Conference on Electrical Contacts (HOLM), pp.1,8, 22-25 Sept. 2013.
- 8 C. D. Patel and G. M. Rebeiz (2012), “A High-Reliability High-Linearity High-Power RF MEMS Metal-Contact Switch for DC–40-GHz Applications,” *IEEE Transactions on Microwave Theory and Techniques* vol 60, pp 3096-3112
- 9 Fei Wang, Xinxin Li, Rong Cheng, Kewei Jiang, and Songlin Feng (2009), “Silicon cantilever arrays with by-pass metal through-silicon-via (TSV) tips for micromachined IC testing probe cards,” *Microelectronics Engineering*, 86, pp. 2211-2216.
- 10 Fei Wang, Xinxin Li, and Songlin Feng (2008), “A MEMS probe-card with 2-D dense-arrayed ‘hoe-shaped’ metal tips”, *Journal of Micromechanics and Microengineering*, Volume 18, Issue 5, 055008 (8 pp).
- 11 K. Kataoka, T. Itoh, T. Suga, K. Inoue (2004), “Contact properties of Ni micro-springs for MEMS probe card,” *Proceedings of the 50th IEEE Holm Conference on Electrical Contacts*, 2004, pp.231-235, 20-23 Sept. 2004
- 12 S. T. Patton, J. S. Zabinski (2005), “Fundamental Studies of Au Contacts in MEMS RF Switches”, *Tribology Letters* vol 18(2), pp 215-230.
- 13 R. A. Coutu Jr, P. E. Kladitis, R. Cortez, R. E. Strawser and R. L. Crane (2006), “Micro-Switches With Sputtered Au, AuPd, Au-On-AuPt, And AuPtCu Alloy Electric Contacts”, *IEEE Trans. Compon. Packag. Technol.* Vol 29 pp 341–9.

-
- 14 L. Chen, Z.J. Guo, N. Joshi, H. Eid, G.G. Adams and N.E. McGruer (2010), "An SPM-Based Contact Tester for Study of Microcontacts," Solid State Sensors, Actuators and Microsystems Workshop 2010, Hilton Head Island, South Carolina, June 6-10, pp. 190-193.
- 15 L. Chen, Z. Guo, N. Joshi, H. Eid, G. Adams and N. McGruer (2012), "An improved SPM-based contact tester for the study of microcontacts", *J. Micromech. Microeng.*, vol 22, 045017.
- 16 M. Walker, C. Nordquist, D. Czaplewski, G. Patrizi, N. McGruer and J. Krim (2010), "Impact of in situ Oxygen Plasma Cleaning on the Resistance of Ru and Au-Ru Based RF Microelectromechanical System Contacts in Vacuum", *Journal of Applied Physics*, vol 107, 084509 (2010).
- 17 D. J. Dickrell, M. T. Dugger (2007), "Electrical Contact Resistance Degradation of a Hot-Switched Simulated Metal MEMS Contact," *IEEE Transactions on Components and Packaging Technologies*, vol.30, no.1, pp.75-80, March 2007.
- 18 Benjamin F Toler, Ronald A Coutu Jr and John W McBride (2013), "A review of micro-contact physics for microelectromechanical systems (MEMS) metal contact switches," *Journal of Micromechanics and Microengineering*, vol. 23, p. 103001, 2013.
- 19 E. J. J. Kruglick (1999), "Micro-relay design, performance, and systems," Ph.D. dissertation, Univ. California Berkeley, Berkeley, CA, 1999.
- 20 R. P. Hennessy, A. Basu, G. G. Adams and N. E. McGruer (2013), "Hot-switched Lifetime and Damage Characteristics of MEMS Switch Contacts", *J. Micromech. Microeng.*, vol 23 055003.
- 21 M. Vincent, S. W. Rowe, C. Poulain, D. Mariolle, L. Chiesi (2010), "Field Emission and Material Transfer in Microswitches Electrical Contacts", *Applied Physics Letters*, vol 97, 263503.
- 22 C. Poulain, A. Peschot, M. Vincent, N. Bonifaci (2011), "A Nano-Scale Investigation of Material Transfer Phenomena at Make in a MEMS Switch," 2011 IEEE 57th Holm Conference on Electrical Contacts (Holm), pp.1,7, 11-14 Sept. 2011.
- 23 Z. Yang, D. Lichtenwalner, A. Morris, J. Krim, and A. Kingon, (2010), "Contact Degradation in Hot/Cold Operation of Direct Contact Micro-Switches", *J. Micromech. Microeng.*, vol 20, 105028.
- 24 P. G. Slade (2008), "The transition from the molten bridge to the metallic phase bridge column arc between electrical contacts opening in vacuum," 23rd International Symposium on Discharges and Electrical Insulation in Vacuum, ISDEIV 2008., vol.1, pp.198,201, 15-19 Sept. 2008.
- 25 F. Pons (2010). "Electrical Contact Material Arc Erosion: Experiments And Modeling Towards The Design of an AgCdo Substitute", PhD dissertation, Georgia Institute of Technology, Atlanta, Georgia, URL: <http://hdl.handle.net/1853/33816>.
- 26 T. Ishida, K. Kakushima, H. Fujita (2013), "Degradation Mechanisms of Contact Point During Switching Operation of MEMS Switch," *Journal of Microelectromechanical Systems*, vol.22, no.4, pp.828,834, Aug. 2013.

-
- 27 P. M. Davidson (1954), “The Growth of the Liquid Bridge in an Electrical Contact”, *Brit. J. Appl. Phys.* vol. 5, pp. 189 – 191.
- 28 R. S. Timsit (2010), “Electromigration in a Liquid Bridge before Contact Break,” *Proceedings of the 56th IEEE Holm Conference on Electrical Contacts (HOLM)*, 2010, pp.1,6, 4-7 Oct. 2010.
- 29 R. Holm, “*Electric Contacts, Theory and Applications*”, 4th edition, Springer-Verlag, New York, 1981.
- 30 Qing Ma, Quan Tran, Tsung-Kuan A. Chou, John Heck, Hanan Bar, Rishi Kant, Valluri Rao (2007), “Metal Contact Reliability Of RF MEMS Switches”, *Proc. SPIE 6463, Reliability, Packaging, Testing, and Characterization of MEMS/MOEMS VI*, 646305 (January 19, 2007).
- 31 K. W. Gilbert, S. Mall, K. D. Leedy, B. Crawford, “A Nanoindenter Based Method for Studying MEMS Contact Switch Microcontacts,” *Proceedings of the 54th IEEE Holm Conference on Electrical Contacts*, 2008, pp.137,144, 27-29 Oct. 2008.
- 32 Esa M. Yunus, J. W. M., and Simon M. Spearing (2009), “The Relationship Between Contact Resistance and Contact Force on Au-Coated Carbon Nanotube Surfaces Under Low Force Conditions”, *IEEE Transactions on components and packaging technologies* vol 32, pp 650-657.
- 33 Z. Yang, D. L., A. Morris, S. Menzel, C. Nauenheim, A. Gruverman, J. Krim and A. I. Kingon (2007), “A New Test Facility for Efficient Evaluation of MEMS Contact Materials”, *Journal of Micromechanics and Microengineering* vol 17, pp 1788-1795.
- 34 Beth L. Pruitt, Member, IEEE, Member, ASME, Woo-Tae Park, and Thomas W. Kenny (2004), “Measurement System for Low Force and Small Displacement Contacts”, *JOURNAL OF MICROELECTROMECHANICAL SYSTEMS*, VOL. 13, NO. 2, pp 220 – 229
- 35 B. Toler, C. Stilson, R. Coutu (2013), “Contact Resistance Evolution of Au-Au Micro-Contacts with Encapsulated Ag Colloids,” *2013 IEEE 59th Holm Conference on Electrical Contacts (HOLM)*, pp.1,8, 22-25 Sept. 2013
- 36 A. Basu, R. Hennessy, G. Adams, N. McGruer (2013), “Leading and trailing edge hot switching damage in a metal contact RF MEMS switch,” *The 17th International Conference on Solid-State Sensors, Actuators and Microsystems (TRANSDUCERS & EUROSENSORS XXVII)*, 2013, pp.514,517, 16-20 June 2013.
- 37 A. Basu, R. Hennessy, G. Adams, N. McGruer (2013), “Reliability in Hot Switched Ruthenium on Ruthenium MEMS Contacts,” *2013 IEEE 59th Holm Conference on Electrical Contacts (HOLM)*, pp.1,8, 22-25 Sept. 2013.
- 38 D. Braun (2003), “Electronic Injection and Conduction Processes for Polymer Devices”, *Journal of Polymer Science Part B: Polymer Physics* vol 41 pp 2622-2629.
- 39 K. Roy, S. Mukhopadhyay, H. Mahmoodi-Meimand (2003), “Leakage Current Mechanisms and Leakage Reduction Techniques in Deep-Submicrometer CMOS Circuits”, *Proceedings of the IEEE* vol 91 pp 305-327.

-
- 40 T. T. Tsong (1991), “Effects of an Electric Field in Atomic Manipulations”, *Phys. Rev. B* vol 44 pp 13703–13710.
- 41 I. Langmuir and K. H. Kingdon (1925), “Thermionic effects caused by Vapours of Alkali metals”, *Proc. Royal Society of Lond. A*, 1 January 1925, **vol. 107 no. 741**, pp 61-79
- 42 Paul.G. Slade, “Electrical Contacts Principles and Applications”, Marcel Dekker Inc, 270 Madison Ave, New York, NY, 1999.
- 43 Robert D. Malucci (2013), “The Impact of Electro-Migration on Various Contact Materials,” 2013 IEEE 59th Holm Conference on Electrical Contacts (HOLM), pp.1,8, 22-25 Sept. 2013.
- 44 T. R. Anthony, “The electromigration of liquid metal inclusions in Si,” *Journal of Applied Physics*, vol.51, no.12, pp.6356,6365, Dec 1980.
- 45 Luc D. Delaney (2006), “A First Report on Electromigration Studies at a Molten Copper-Aluminum Railgun Contact”, M.S. Thesis, Naval Postgraduate School, Monterey, California, URL: <http://hdl.handle.net/10945/2511>.
- 46 R. Hennessy, N.E. McGruer and G.G. Adams (2012), “Modeling of a Thermal-Electrical-Mechanical Coupled Field Contact”, *Journal of Tribology* vol 134, 041402, 8 pp.
- 47 Young-Chang Joo, Tae-Youl Yang, Ju-Young Cho, and Yong-Jin Park (2012), “Electromigration in Molten-phase Ge₂Sb₂Te₅ and Effects of Doping on Atomic Migration Rate”, *Journal of the Korean Ceramic Society* vol 49 pp 43-47.
- 48 Henry E. Duckworth(1960), “Electricity and Magnetism”, New York: Holt, Rinehart and Winston, pp. 182-184.
- 49 S. Fostner, A. Tekiel, J. M. Topple, Y. Miyahara and P. Grutter (2011), “Field deposition From Metallic Tips onto Insulating Substrates”, *Nanotechnology*, vol 22 no 46, 465301.
- 50 Hajime Koyanagi, Sumio Hosaka, Ryo Imura, and Masataka Shirai (1995), “Field Evaporation of Gold Atoms onto a Silicon Dioxide Film by Using an Atomic Force Microscope”, *Applied Physics Letters*, vol 67, pp 2609-2611 (1995).
- 51 M. Calleja, M. Tello, J. Anguita, F. García, and R. García (2011), “Fabrication of Gold Nanowires on Insulating Substrates by Field-Induced Mass Transport” *Applied Physics Letters*, vol 79, pp 2471-2473.